OXFORD
SOT | Society of Toxicology
www.toxsci.oxfordjournals.org

TOXICOLOGICAL SCIENCES, 147(2), 2015, 425–435

doi: 10.1093/toxsci/kfv138
Advance Access Publication Date: July 2, 2015
Research Article

Ah Receptor Signaling Controls the Expression of Cardiac Development and Homeostasis Genes

Vinicius S. Carreira,* Yunxia Fan,* Qing Wang,* Xiang Zhang,* Hisaka Kurita,* Chia-I. Ko,* Mindi Naticchioni,† Min Jiang,† Sheryl Koch,† Mario Medvedovic,* Ying Xia,* Jack Rubinstein,† and Alvaro Puga*,[1]

*Department of Environmental Health and Center for Environmental Genetics and †Department of Internal Medicine, Cardiology Division, University of Cincinnati College of Medicine, Cincinnati, Ohio 45267

[1]To whom correspondence should be addressed at Department of Environmental Health and Center for Environmental Genetics,University of Cincinnati College of Medicine, Cincinnati, Ohio 45267. Fax: (513) 558-0925. E-mail: alvaro.puga@uc.edu

ABSTRACT

Congenital heart disease (CHD) is the most common congenital abnormality and one of the leading causes of newborn death throughout the world. Despite much emerging scientific information, the precise etiology of this disease remains elusive. Here, we show that the aryl hydrocarbon receptor (AHR) regulates the expression of crucial cardiogenesis genes and that interference with endogenous AHR functions, either by gene ablation or by agonist exposure during early development, causes overlapping structural and functional cardiac abnormalities that lead to altered fetal heart physiology, including higher heart rates, right and left ventricle dilation, higher stroke volume, and reduced ejection fraction. With striking similarity between AHR knockout ($Ahr^{-/-}$) and agonist-exposed wild type ($Ahr^{+/+}$) embryos, *in utero* disruption of endogenous AHR functions converge into dysregulation of molecular mechanisms needed for attainment and maintenance of cardiac differentiation, including the pivotal signals regulated by the cardiogenic transcription factor NKH2.5, energy balance via oxidative phosphorylation and TCA cycle and global mitochondrial function and homeostasis. Our findings suggest that AHR signaling in the developing mammalian heart is central to the regulation of pathways crucial for cellular metabolism, cardiogenesis, and cardiac function, which are potential targets of environmental factors associated with CHD.

Key words: Ah receptor; cardiogenesis; congenital heart disease; mitochondrial dysfunction; NKX2-5

Congenital heart disease (CHD) is the most common congenital abnormality and one of the leading causes of newborn death in developed and many developing countries. Notwithstanding a wealth of emerging scientific information, the precise etiological basis underlying the majority of CHD cases remain elusive. Recent epidemiologic studies estimate that <15% of cases of CHD can be traced to known causes of Mendelian inheritance (van der Bom *et al.*, 2011), suggesting the likelihood that environmental agents operative at the time of heart formation may be critical etiological contributors to the disease (Hinton, 2013; Lage *et al.*, 2012; Vecoli *et al.*, 2014). A multifactorial pathogenesis with interplay between genetic, epigenetic, and environmental factors would be consonant with the tenets of the theory of the Developmental Origins of Health and Disease, which postulates that the environment in the uterus enduringly shapes the structure, function, and metabolism of the adult organism (Barker, 2007). Accordingly, damage resulting from environmental insults during fetal life may be at the heart of congenital and adult onset cardiac diseases.

Some such insults may be the consequence of exposure to xenobiotic environmental agents that signal through the aryl hydrocarbon receptor (AHR). Developmental interference with endogenous AHR functions has been shown to adversely affect the cardiovascular system in various experimental models, both *in vitro* (Jones and Kennedy, 2009; Wang *et al.*, 2013) and *in vivo* (Abbott *et al.*, 1999; Aragon *et al.*, 2008; Carro *et al.*, 2013; Dalton *et al.*, 2001; Hofsteen *et al.*, 2013; Puga, 2011; Yoshioka *et al.*, 2011), and have implicated the AHR in the etiology of

cardiovascular disease. Significantly, maternal exposure to environmental teratogens was proposed more than 50 years ago to contribute to and potentially explain a large proportion of CHD (Nora, 1968), yet little direct evidence has since been developed that tested this hypothesis.

Cardiogenesis is the product of the precise orchestration of innumerable gene networks regulating developmental commitments toward cellular differentiation, migration, proliferation, and death (Rana *et al.*, 2013; Srivastava and Olson, 2000; Van Vliet *et al.*, 2012). In this setting, the developing heart has been found to be exquisitely sensitive to AHR disruption (Aragon *et al.*, 2008; Puga, 2011; Thackaberry *et al.*, 2005) likely due to the critical endogenous role of this receptor in embryogenesis. Genome-wide studies in mouse embryonic stem cells have shown that disruption of endogenous AHR expression perturbs cardiomyocyte differentiation, underscoring a critical role for the receptor in a complex regulatory target network for cardiogenesis and cardiovascular homeostasis (Wang *et al.*, 2013). The endogenous AHR signaling has also been shown to carry out enduring functions in postnatal cardiac physiology, such as cardiac sufficiency and blood pressure regulation (Lund *et al.*, 2008; Sauzeau *et al.*, 2011; Zhang, 2011) and cardiovascular pathology (Dabir *et al.*, 2008). These observations suggest that AHR contributes at multiple levels to global cardiovascular health, though whether cardiac pathology can be experimentally linked to gestational disruption of the AHR signaling pathway remains to be determined.

As a ligand-activated transcription factor and a member of the basic-region-helix-loop-helix PER/ARNT/SIM (bHLH-PAS) superfamily, the AHR is classically known to mediate the ligand-dependent induction of xenobiotic metabolism programs, such as controlled by the CYP1 family of cytochrome P450s and several phase II detoxification enzymes (Puga, 2011). Members of the bHLH-PAS protein superfamily differentially regulate various signaling pathways related to development and homeostasis (Kewley *et al.*, 2004). The AHR pathway is further implicated in the regulation of several developmental and homeostatic biological processes, such as immune response, growth factor signaling, cell cycle proliferation, differentiation, arrest, and apoptosis (Aragon *et al.*, 2008; Puga *et al.*, 2009; Quintana and Sherr, 2013; Thackaberry *et al.*, 2005). Importantly, the AHR is also a key environmental sensor (Furness *et al.*, 2007), and, when activated by exogenous ligands during mouse development, recapitulates some of the phenotypes observed in mice with constitutive ablation of the *Ahr* gene (Aragon *et al.*, 2008).

TCDD (2,3,7,8-tetrachlorodibenzo-*p*-dioxin; dioxin) is one such exogenous ligand and one of the most potent AHR agonists (Schmidt and Bradfield, 1996). After ligand-induced activation, AHR induces the expression of its target genes, followed by proteasome-dependent degradation leading to overall depletion of AHR in the cell (Davarinos and Pollenz, 1999; Giannone *et al.*, 1998). It is hypothesized that 'postexposure AHR downregulation' may mimic an AHR-null condition. Alternatively, it is speculated that the exogenous (xenobiotic) ligands may compete with the endogenous (physiological) ligands, thereby diverting AHR from its normal biological functions (Furness and Whelan, 2009). Which of the endogenous AHR functions are perturbed by toxic chemicals remains to be determined.

To address the hypothesis that developmental disruption of the endogenous AHR program by either constitutive ablation or by an exogenous ligand exposure would result in cardiac abnormalities *in vivo*, we sought to characterize at key cardiogenesis developmental windows the molecular, structural, ultrastructural, functional, and pathological cardiac phenotypes of naïve *Ahr* knockout mice ($Ahr^{-/-}$) embryos and either naive wild-type ($Ahr^{+/+}$) embryos or $Ahr^{+/+}$ embryos exposed *in utero* to a potent AHR agonist.

MATERIALS AND METHODS

Animals and treatments. All experiments were conducted using the highest standards of humane care in accordance with the NIH Guide for the Care and Use of Laboratory Animals and were approved by the University of Cincinnati Institutional Animal Care and Use Committee. Age-matched $Ahr^{+/+}$ and $Ahr^{-/-}$ C57BL/6J female mice were mated overnight with $Ahr^{+/+}$ and $Ahr^{-/-}$ C57BL/6J male mice, respectively. Maternal gestational exposure to the prototypical AHR ligand TCDD was performed via oral gavage at key developmental time points as previously described (Wang *et al.*, 2013) and is illustrated in detail in Supplementary Figure S1A. Dams were treated by oral gavage with either corn oil (vehicle) or with TCDD at doses of 0.1, 0.5, 1, 2.5, 5, or 50 μg/kg, which based on previous determinations are estimated to correspond to 0.034, 0.17, 0.34, 0.85, 1.7, and 17 ng, respectively, to the embryos (Weber and Birnbaum, 1985). For the sake of clarity, all developmental samples are referred to as embryos, even though the later time points used would technically qualify for the term fetus. Embryo samples were collected on E13.5, E15.5, and E18.5. To assess for potential toxic effects from this exposure, maternal and F1 body and organ weights were measured and litter size and sex ratios recorded. The overall outcomes of gestational AHR disruption, be it by receptor ablation or potent agonist exposure, are detailed in Supplementary Figure S1B-I.

Organ and embryo weights. Following euthanasia, gravid *uteri* were immediately harvested and excess tissue trimmed to isolate individual embryos free of extraembryonic membranes. Embryos were gently blotted to remove excess fluids and weighed using a high definition scale. The maternal and embryo liver weights were determined by isolating the liver free of other tissues, gently blotting to remove excess fluids and weighing. Dry embryo body and embryo heart weights were determined following 48-h incubation in a drying oven at 60°C. When appropriate, organ weights were normalized to body weight.

Histology, immunohistochemistry, and microscopy. Tissues samples were fixed for 48 h in freshly prepared 4% paraformaldehyde at 4°C (Sigma-Aldrich), rinsed in serial ethanol dilutions, and then routinely processed for histology. Immunostaining and routine hematoxylin and eosin (H&E) staining was performed using standard protocols as previously described (Mongan *et al.*, 2008). For immunohistochemistry, rabbit polyclonal primary antibodies against AHR (SA-210 Enzo), NKX2-5 (Ab35842, Abcam), and Ki-67 (anti-rabbit, Millipore) were used. Immunostaining quantification was performed using the color deconvolution plugin and threshold functions of the ImageJ 1.47h (National Institutes of Health) to determine the percentage of nuclei labeled (% positive index). Immunohistochemical analyses were performed on 4–5 embryos per experimental condition. Morphometrical analyses were carried out in 3 serial sections of at least 4–5 embryos per experimental condition using the Zen morphometry suite (Blue Edition version 1.0.0.0, Carl Zeiss Microscopy). Briefly, for each section manual measurements using the line function were taken of the ventricle wall perpendicular to the apex-base axis of the heart to include the trabecular and compact

myocardium (total thickness) or only compact myocardium (compact ventricle thickness).

Transmission electron microscopy. At least 3 hearts per treatment group were immediately fixed in phosphate-buffered 3% glutaraldehyde for 24 h and submitted to the Pathology Research Core at Cincinnati Children's Hospital Medical Center for sample processing and sectioning for electron microscopic examination. Samples were washed 3 times in 0.1 M cacodylate buffer and postfixed in 1% osmium tetroxide buffered with cacodylate, pH 7.2, at 4°C for 1 h. After dehydration in serial alcohol and propylene oxide solutions, samples were infiltrated with and embedded in LX112. Thin sections were stained with uranyl acetate and lead citrate. Imaging was performed on a transmission electron microscope (7600; Hitachi). Five nonoverlapping ultraphotomicrographs per grid were taken at ×8000, ×25 000, and ×70 000 magnifications and evaluated using Image J 1.47h software.

Mitochondria quantification. The relative amounts of embryo heart mitochondria (ratio of mitochondrial DNA [mtDNA] to nuclear DNA [nDNA]) were determined using a RT-PCR method as previously described (Stites *et al.*, 2006). The targets were the genes coding for the nuclear cytochrome P450 *Cyp1a1* and for the mitochondrial nicotinamide adenine dinucleotide dehydrogenase-5 (*Nd5*). Primers for the *Cyp1a1* promoter region at −0.9 kb were: forward: 5′-AGGCTCTTCTCACGCAACTC-3′; reverse: 5′-TAAGCCTGCTCCATCCTCTG-3′. Primers for *Nd5* were: forward 5′-TGG ATG ATG GTA CGG ACG AA-3′; reverse 5′-TGC GGT TAT AGA GGA TTG CTT GT-3′.

RNA.seq analysis. Embryo hearts were microdissected into right atrium, left atrium, and ventricles with the assistance of a dissecting microscope (Supplementary Fig. S4A). Individual samples were stored in 200 µl of RNA-Later at −80°C until RNA extraction. Total RNA was extracted with the RNeasy Mini Kit (QIAGEN) with Proteinase K and DNAse steps. All steps of library construction, cluster generation, and HiSeq (Illumina) sequencing were performed with biological triplicate samples by the Genomics Sequencing Core of the Department of Environmental Health, University of Cincinnati. Differential gene expression analyses between $Ahr^{+/+}$ and $Ahr^{-/-}$ embryos or between AHR ligand-exposed and naïve $Ahr^{+/+}$ embryos were performed separately at each of the 3 different developmental time points (E13.5, E15.5, and E18.5). Statistical analyses were performed to identify differentially expressed genes for each comparison using the negative-binomial model of read counts as implemented in the Biocondoctor DESeq package. Significant genes were selected based on a false-discovery rate-adjusted *P*-value < .0001. RNA.seq data were further analyzed using Ingenuity Pathway Analysis (IPA; Ingenuity Systems, http://www.ingenuity.com).

Embryo (in utero) echocardiography. To evaluate for functional abnormalities we performed a full high-frequency echocardiographic study of the embryos *in utero* at E15.5. The study was carried out as previously described (Srinivasan *et al.*, 1998) using the Vevo 2100 Ultrasound system equipped with a MS700 30–70 MHz probe and postprocessed at a separate workstation (Visualsonic, Vevo 2100, v1.1.1 B1455) by a blinded investigator (an illustrative example is shown in Supplementary Fig. S2). The B-mode, color, and Doppler images were analyzed for valvular function and structural abnormalities, while the M-mode images were postprocessed for cardiac functional analysis including ventricular size, ejection fraction, and cardiac output.

RESULTS

The AHR Is Largely Nuclear During Early Differentiation

To determine whether AHR plays a role in cardiogenesis, we probed matching sections of hearts from mouse embryos exposed to TCDD or vehicle control for AHR expression at key cardiogenesis time points. AHR was detected at embryonic day E13.5, the earliest time point measured. In vehicle-exposed controls, ∼12% of the ventricular cells were positive for AHR expression, which was mostly localized to the nucleus of cells lining the developing epicardium, with little or no evidence of cytoplasmic localization (Figs. 1A and 1B). In TCDD-exposed embryos, the number of AHR positive cells was reduced to approximately one-half of the control value (Supplementary Fig. S3), a change consistent with the notion that ligands promote receptor down-regulation. At E15.5, nuclear AHR-positive cells decreased significantly both in control and TCDD-treated embryos and by E18.5 the amount of AHR was much less abundant in the nucleus (Figs. 1A and 1B). The detection of AHR in the nucleus of early developing hearts suggests that the AHR functionally contributes to heart formation during a critical window of development and that exogenous ligands, which attenuate the nuclear localization of the endogenous AHR at this developmental time, may interfere with the AHR endogenous role in cardiogenesis.

Developmental Disruption of AHR Signaling Alters the Structure of the Developing Myocardium

Activation of the AHR pathway by exogenous ligands has been associated with disruption of developmental and homeostatic biological processes, including growth factor signaling, cell cycle proliferation, differentiation, arrest, and apoptosis (Puga *et al.*, 2009). To determine whether altered AHR signaling during cardiogenesis caused structural abnormalities in the developing heart, we examined embryonic hearts from naïve $Ahr^{-/-}$ mice and from wild-type mice gestationally exposed to TCDD or to vehicle. Exposure to TCDD *in utero* resulted in decreased cross-sectional left wall thickness at E13.5, E15.5, and E18.5, whereas *Ahr* ablation decreased left wall thickness at E13.5 and E15.5, but not E18.5 (Fig. 2A). Histomorphometric assessment of serial sections showed that $Ahr^{-/-}$ and ligand-exposed embryos had thinner left ventricular myocardium at all measured time points, except at E18.5 for $Ahr^{-/-}$ (Fig. 2B), despite the fact that these hearts had a relative increase in the thickness of the left ventricle compact myocardium (Fig. 2C and Supplementary Fig. S4). Ligand-exposed $Ahr^{+/+}$ embryos had decreased heart weight relative to body weight (Fig. 2D). The $Ahr^{-/-}$ embryos had reduced heart weight at E13.5, but increased heart weight at E15.5, and unchanged at E18.5. Altogether, these data support the conclusion that disruption of AHR signaling *in utero* alters the developing myocardium structure, composition, and mass.

To determine whether the observed decreases in myocardium mass were the consequence of a measurable decrease in cell proliferation, we probed sections of embryonic heart tissue for expression of the Ki-67 antigen, a proxy for cellular proliferation (Scholzen and Gerdes, 2000). The Ki-67 index was determined throughout the myocardium to include right and left atria and ventricles, as well as the interventricular septum. Exposure of $Ahr^{+/+}$ mice to ligand induced a significant increase in cellular proliferation across subanatomical areas of the

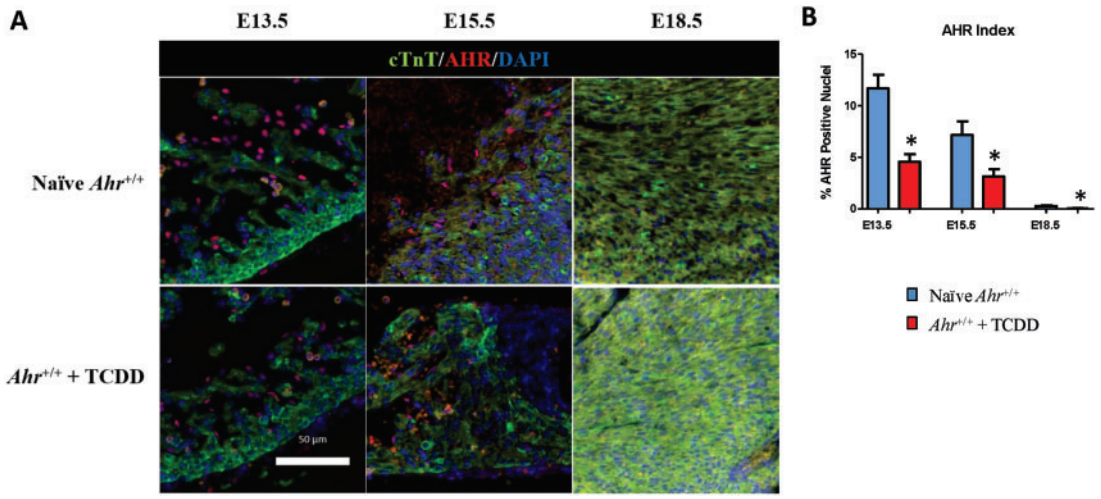

FIG. 1. AHR localization during early heart formation. A, Five-micrometer sections of embryonic hearts collected at E13.5, E15.5, and E18.5 from $Ahr^{+/+}$, naïve or exposed to AHR ligand (TCDD) *in utero*, were used for immunofluorescent detection of AHR (red) and cardiac troponin T (green). Staining with DAPI identifies the nuclei. AHR, aryl hydrocarbon receptor; cTnT, cardiac troponin T; DAPI, nuclei; scale bar = 50 μm. B, Quantification of nuclear localization of AHR (AHR Index) at the indicated embryonic developmental times. The AHR index is shown as the mean percent positive nuclei ± SEM; *$P \leq .05$. Full color version available online.

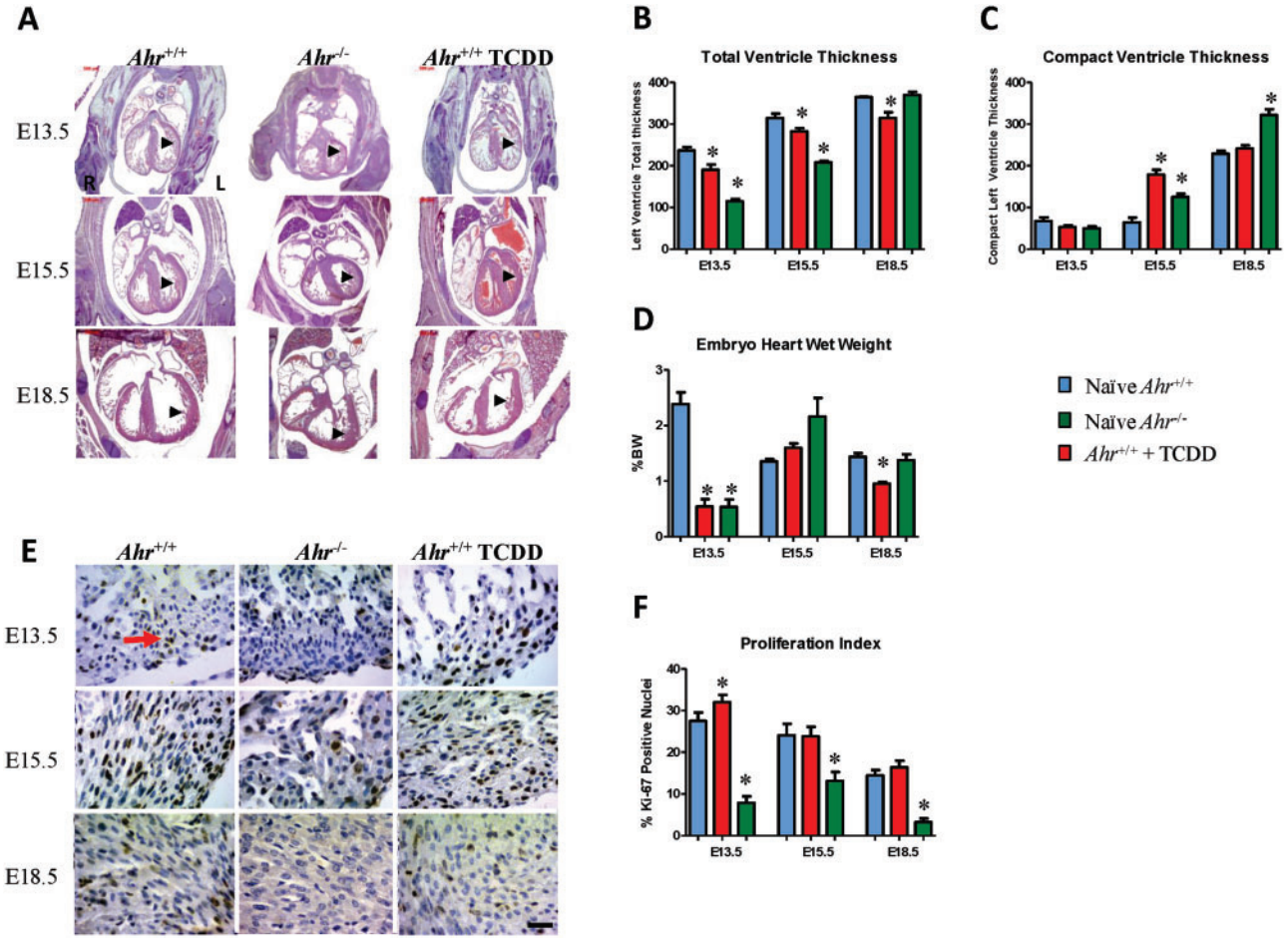

FIG. 2. Structural changes in the developing myocardium. A, Sections from the same embryos used in Fig. 1 were used for histomorphometric assessment of the developing myocardium. H&E stain is shown. Scale bar = 500 μm. B, C, Quantification of histomorphometric ventricular measurements at the indicated embryonic developmental times. Shown is the mean ± SEM; *$P \leq .05$. D, Embryo heart wet weights relative to body weight at the indicated embryonic developmental times shown as the percent of mean body weight ± SEM; *$P \leq .05$. E, Sections from the same embryos used in Fig. 1 were used for immunohistochemical detection of Ki-67 as a proxy for cellular proliferation (golden-brown nuclei—arrow) and counterstained with Harris hematoxylin. Scale bar = 50 μm. F, Quantification of nuclear localization of Ki-67 (Proliferation Index) at the indicated embryonic developmental times. The proliferation index is shown as the mean percent positive nuclei ± SEM; *$P \leq .05$. Full color version available online.

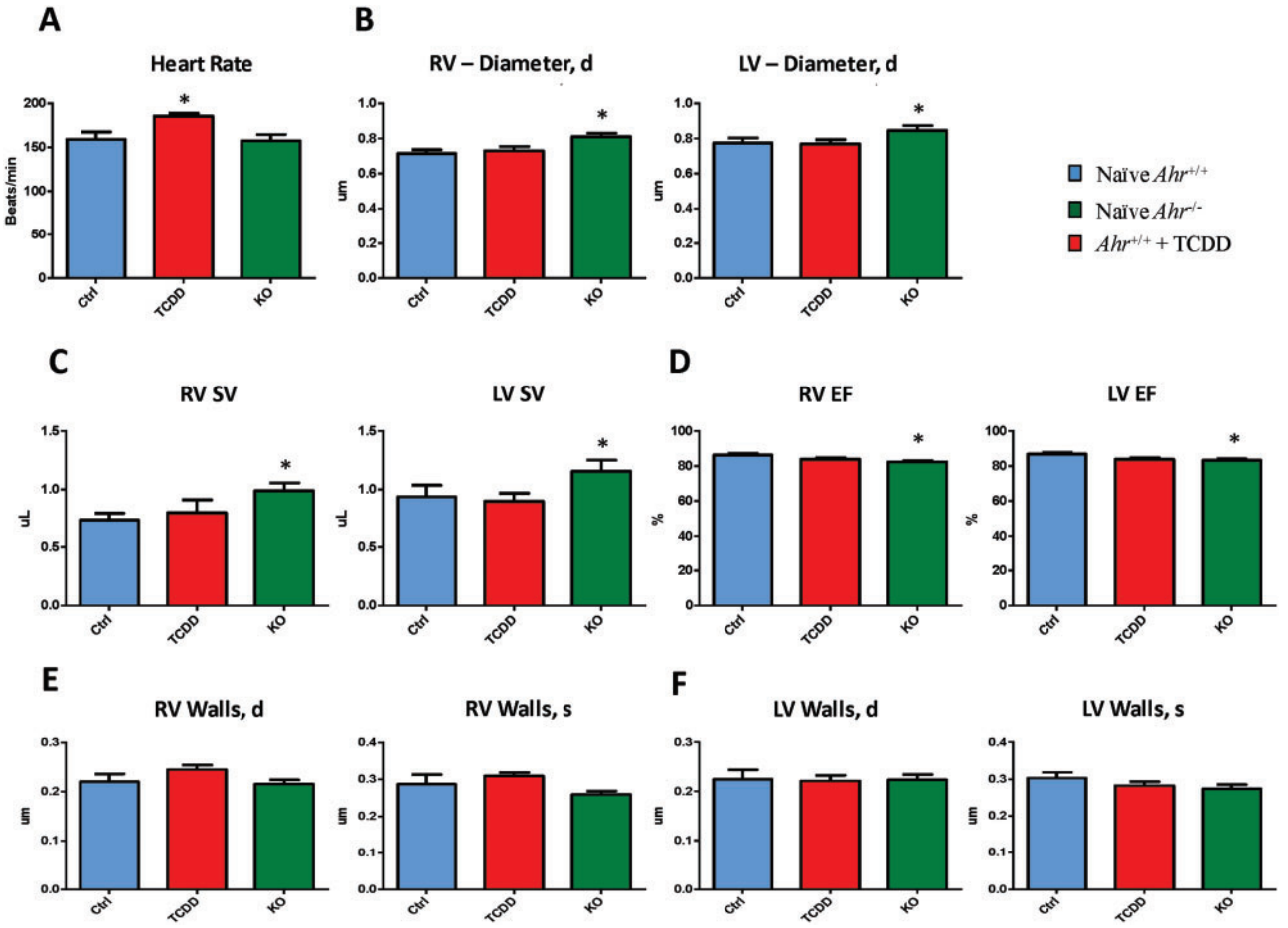

FIG. 3. Effect of developmental AHR disruption on embryonic heart function. $Ahr^{+/+}$ embryos, naïve (*blue*) or exposed to ligand (*red*) *in utero*, and $Ahr^{-/-}$ embryos (*green*) were subjected to *in utero* echocardiography at E15.5 to assess heart rate (A), ventricular diameters (B), right ventricle stroke volume (C), left ventricle stroke volume (D), ventricular ejection fraction (D), right ventricle diastolic and systolic wall thickness (E), and left ventricle diastolic and systolic wall thickness (F). The histograms represent the mean ± SEM of the determinations on 3–5 l. $^*P \leq .05$. Full color version available online.

embryo hearts at E13.5, with no significant differences at E15.5 and E18.5. On the other hand, $Ahr^{-/-}$ hearts showed significantly decreased proliferation indices at all time points tested (Figs. 2E and 2F). Masson's trichrome histochemistry revealed no significant differences in interstitial collagen deposition (data not shown), suggesting that remodeling of the interstitial matrix was not a major contributor to the observed effects. The large differences that we observe in proliferation indices suggest that the alterations in myocardial composition and mass could be related to the observed decrease of cardiomyocyte proliferation in $Ahr^{-/-}$ hearts, but less so in hearts of AHR ligand-exposed mice.

Developmental AHR Disruption Affects Embryonic Heart Function

To ascertain whether developmental AHR disruption would deter embryonic heart function, we sought to determine if and to which extent echocardiographic parameters of heart physiology were altered by genetic or functional disruption of the AHR. Using *in utero* echocardiography at E15.5, we found that AHR ligand exposure was associated with significantly higher heart rates as compared with those in naïve hearts (Fig. 3A). Conversely, ablation of the *Ahr* gene was associated with significant right and left ventricle dilation (Fig. 3B), higher stroke volumes (Fig. 3C), and reduced ejection fraction (Fig. 3D) relative to naïve hearts. Trends that did not reach statistical significance were also noted for decreased ventricle wall thickness with either ablation of the *Ahr* gene or AHR ligand exposure (Figs. 3E and 3F), consistent with the observation of decreases in embryonic heart weight and histological evidence of myocardial thinning. Altogether, *in utero* echocardiographic assessment of embryonic hearts identified significantly altered parameters and trends preluding a decrement in cardiovascular function, which although not presently overt, occurs at a critical time of embryonic development.

Interference With AHR Signaling Disrupts the Expression of Key Networks Involved in Cardiogenesis and Cardiac Homeostasis

The structural and functional changes in the embryo hearts resulting from *Ahr* ablation or activation by ligand support the hypothesis that the AHR may have a regulatory role in cardiogenesis, to the extent that disruption of differential AHR signaling causes the morphological changes observed. To identify and characterize which AHR-regulated genes and pathways were involved in heart development, we carried out RNA next-generation sequencing (RNA.seq) of naïve $Ahr^{+/+}$, $Ahr^{-/-}$, and ligand-exposed $Ahr^{+/+}$ embryonic hearts, at the 3 distinct developmental milestones in cardiogenesis that we had followed structurally. For these analyses, we studied left atrium, right atrium, and ventricles separately (Supplementary Fig. S5A).

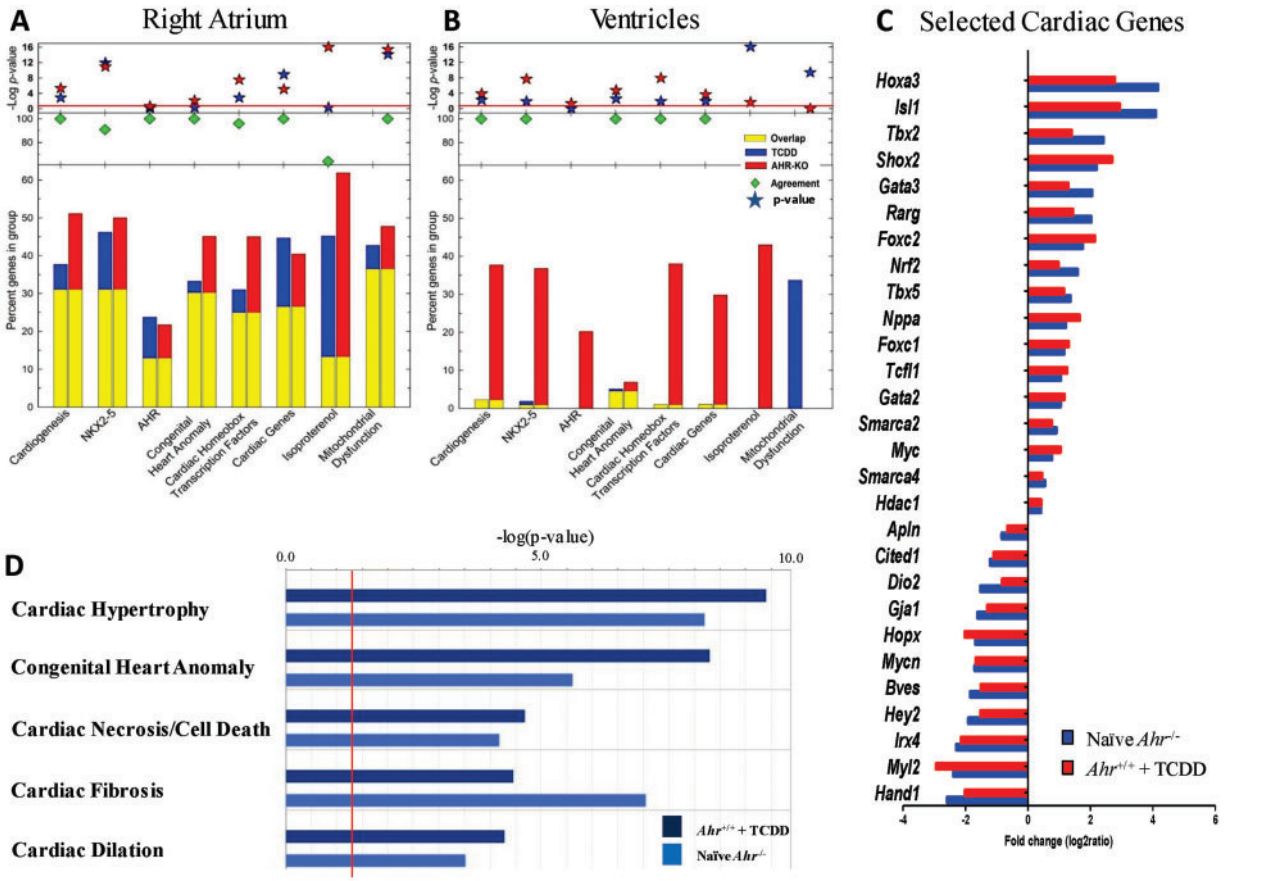

FIG. 4. AHR signaling networks involved in cardiogenesis and cardiac homeostasis. A, The fraction of genes significantly altered in the right atrium of both $Ahr^{-/-}$ and TCDD-exposed $Ahr^{+/+}$ mice (*yellow bars*) or either solely $Ahr^{-/-}$ (*red bars*) or solely TCDD-exposed $Ahr^{+/+}$ (*blue bars*) mice is shown for genes in each of the ontogeny pathways indicated in the abscissa. The *green diamonds* indicate the percent of genes that are in common between $Ahr^{-/-}$ and TCDD-exposed $Ahr^{+/+}$. *Red and blue stars* represent the −log(*P*-value), as a measure of the significance of the observation. B, Same analysis as in (A) for the results with the ventricles. C, Selected list from genes in section (A) of highly concordant genes from $Ahr^{-/-}$ and ligand-exposed $Ahr^{+/+}$ embryo hearts with critical roles in cardiogenesis, and CHD. D, Differentially expressed Ingenuity IPA networks comparison between $Ahr^{-/-}$ embryo hearts (*light blue*) and ligand-exposed $Ahr^{+/+}$ (*dark blue*). The vertical *red line* marks the threshold of statistical significance, as denoted by −log(*P*-value). Full color version available online.

Loss of the *Ahr* gene de-repressed overall gene expression, as $Ahr^{-/-}$ embryo hearts generally had higher numbers of differentially expressed genes compared with ligand-exposed $Ahr^{+/+}$ hearts. Overall, the majority of differentially expressed genes in either ligand-exposed $Ahr^{+/+}$ or $Ahr^{-/-}$, relative to naïve $Ahr^{+/+}$ hearts, were observed at the E15.5 time point in the right atrium. The ventricles showed few differentially expressed genes after ligand exposure and both compartments, ventricles and atria, showed fewer changes at E18.5 (Supplementary Fig. S5B). Differential expression in the left atrium relative to the right atrium was more limited at all 3 time points (Supplementary Fig. S6). Functional annotation of the genes significantly altered at E15.5 in the right atrium and ventricles of $Ahr^{-/-}$ and in ligand-exposed $Ahr^{+/+}$ embryos indicated that a large subset of these genes belong to biologically relevant pathways related to heart formation and function. Specifically, these were pathways implicated in cardiogenesis, NKX2-5 signaling, AHR signaling, congenital heart anomalies, homeobox cardiac transcription factors, cardiac homeostasis and function, and mitochondrial dysfunction (Figs. 4A and 4B). Remarkably, the identity and the direction—induction or repression—of gene expression changes in the E15.5 right atria (Fig. 4A) were strikingly similar between $Ahr^{-/-}$ and ligand-exposed $Ahr^{+/+}$embryos.

Further analysis of RNA.seq data on the basis of the biological relevance of the differentially expressed genes revealed significant ontogenies populated by genes, such as *Shox2, Tbx2, Tbx5, Nppa, Gja1, Hey2, Irx4, Myl2,* and *Hand1,* that were highly concordant between $Ahr^{-/-}$ and TCDD-exposed $Ahr^{+/+}$ mice, all playing critical roles in cardiogenesis and CHD. A high degree of directional and identity overlap was observed among these selected critical cardiogenesis genes (Fig. 4C and Supplementary Table S1). Collectively, differentially expressed genes populated Ingenuity IPA's networks belonging to, among others, cardiac hypertrophy, congenital heart anomaly, cardiac necrosis/cell death, cardiac fibrosis, and cardiac dilation (Fig. 4D and Supplementary Fig. S7). It appears that in the developing heart, receptor ablation or its activation by exogenous ligands similarly disrupt the molecular networks involved in heart formation and function. Seemingly, the changes in embryonic heart transcriptome resulting from *Ahr* ablation or ligand-exposure disrupt common molecular features and pathways that direct cardiac function with a high degree of overlap and directional agreement, especially during development of the right atrium at E15.5.

Developmental AHR Ligand Exposure Reduces the Transcriptional Activity of NKX2-5 Within the Developing Heart

Transcriptome sequencing of embryonic heart mRNAs revealed that AHR disruption resulted in differential expression of the NKX2-5 signaling network, in agreement with our laboratory recent report that developmental loss of AHR homeostasis, as

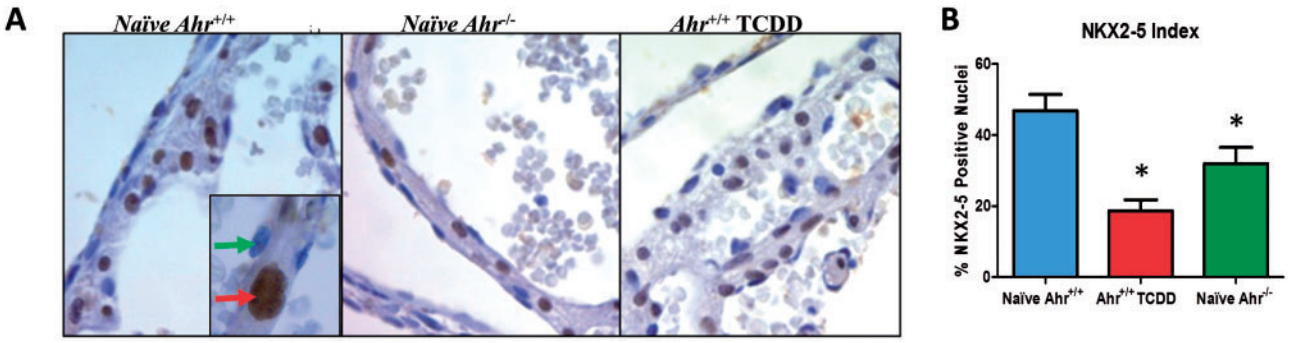

FIG. 5. AHR regulates NKX2-5 expression in the developing heart. A, Higher digital magnification of 5-μm sections of embryonic left atrium collected at E15.5 from $Ahr^{-/-}$ and $Ahr^{+/+}$ either naïve or exposed to TCDD *in utero*, used for immunohistochemical detection of NKX2-5 (DAB-positive nucleus shown by *red arrow* in inset; negative nucleus shown by *green arrow*). Harris hematoxylin counterstained. B, Quantification of NKX2-5-positive nuclei relative to total nuclei at the indicated embryonic developmental times. The NKX2-5 index is shown as the mean percent NKX2-5-positive nuclei ± SEM; *$P \leq .05$. Full color version available online.

caused by exposure to ligand, affects differentiation of ES cells into cardiomyocytes by disrupting the expression of key homeobox regulators, including *Nkx2-5* (Wang *et al.*, 2013). The homeodomain factor *Nkx2-5* is a central regulator of cardiogenesis that specifies the spatial definition, formation, and maintenance of heart structures (Lints *et al.*, 1993; Schwartz and Olson, 1999). The critical role that this gene plays in cardiogenesis is attested to by the fact that *Nkx2-5* hypomorphic mice recapitulate human CHD and that mutations in the homologous *NKH2-5* human gene are commonly found in human CHD cases (Prall *et al.*, 2007). We therefore sought to determine whether *in vivo* gestational disruption of AHR homeostasis would also affect the regulation of *Nkx2-5* expression at the transcription and protein expression levels. Analysis of the right atrium transcriptomes of $Ahr^{-/-}$ and ligand-exposed $Ahr^{+/+}$ revealed a high degree of similarity of both profiles (Supplementary Table S2) with the previously published cardiac transcriptome of *Nkx2-5* mutant mice (Prall *et al.*, 2007). The common pattern, involving key cardiogenesis genes, was characterized by decreased expression of *Nppb, Myl2,* and *Irx4* and increased expression of *Igfbp5, Pdgfra, Tnc, Isl1, Tbx5,* and *Fgf10*. Immunohistochemical staining of embryonic hearts at E15.5 showed a significant decrease of the number of NKX2-5 positive nuclei in embryonic hearts of $Ahr^{-/-}$ and of ligand-exposed $Ahr^{+/+}$ mice (Fig. 5A quantified in Fig. 5B; additional compartment-specific NKX2-5 expression is shown in Supplementary Fig. S8). Collectively, these data indicate that gestational AHR receptor ablation or its activation by ligand exposure is responsible for decreased nuclear localization of the cardiogenic transcription factor NKX2-5, and the consequent disruption of the *Nkx2-5* signaling network.

Developmental AHR Disruption Affects Mitochondria Structure and Abundance

Transcriptome responses in $Ahr^{-/-}$ and in ligand-exposed $Ahr^{+/+}$ embryo hearts showed the significant down-regulation of mitochondrial function pathways (Fig. 6A) and genes controlling critical biological processes involving energy generation and handling, such as oxidative phosphorylation (Fig. 6B) and the TCA cycle (Fig. 6C) were significantly down-regulated. Moreover, mitochondrial Complexes I through V were collectively suppressed in both $Ahr^{-/-}$ (Supplementary Fig. S9) and ligand-exposed $Ahr^{+/+}$ embryo hearts (Supplementary Fig. S10). As in the case of cardiac development genes, the identity and direction of change of mitochondrial function genes were largely identically affected in embryo hearts of *Ahr* knockout and ligand-treated $Ahr^{+/+}$ mice. Notably, at a time when expression of genes controlling oxidative energy metabolism must increase to cope with increased energy requirements in the developing embryo (Li *et al.*, 2014) the effect of either *Ahr* ablation or ligand exposure to $Ahr^{+/+}$ mice could greatly impair mitochondrial homeostasis in the embryonic heart.

To study the structural consequences of mitochondrial dysfunction, embryo hearts at E13.5, E15.5, and E18.5 were examined for the abundance and quality of heart mitochondria. A measure of the ratio of mtDNA to nuclear DNA, coupled with ultrastructure studies, revealed a higher abundance of mitochondria in hearts of $Ahr^{-/-}$ and ligand-exposed $Ahr^{+/+}$. Specifically, at E15.5 and E18.5, the copy number of mitochondria was twice and 3 times higher, respectively, in $Ahr^{-/-}$ and in ligand-exposed $Ahr^{+/+}$ than in naïve $Ahr^{+/+}$ (Fig. 7A). Ultrastructurally, the increased mitochondria numbers was also evident by their higher density within the embryonic cardiomyocyte sarcoplasm (Fig. 7B). Furthermore, individual or clusters of mitochondria showed ultrastructural features of stress and degeneration, as evidenced by focal to global swelling, loss of matrix density, as well as cristae unpacking, disorganization, and cristolysis which appeared to affect higher numbers of mitochondria in ligand-exposed $Ahr^{+/+}$ hearts. These changes were observed at E13.5 in ligand-exposed $Ahr^{+/+}$ hearts as well as at E15.5 and E18.5 in either ligand-exposed $Ahr^{+/+}$or $Ahr^{-/-}$ embryo hearts (Fig. 7B). Overall, these data indicate that the mitochondrial dysfunction postulated on the basis of transcriptome analyses correlated with and was substantiated by quantitative and qualitative structural changes to the embryonic heart mitochondria. Alterations in mitochondria abundance and ultrastructure being likely compensatory responses to the suppressed mitochondrial functional networks.

DISCUSSION

In this study we show that interference with endogenous AHR functions during early development, through gene ablation or exposure to TCDD, perturbs cardiogenesis and leads to molecular and structural cardiac abnormalities, and departure from functional homeostasis. These developmental cardiac effects take place at TCDD doses well below the well-characterized teratogenic doses that cause cleft palate and hydronephrosis. By targeting the post-implantation period of organogenesis, gestational exposure to ligand was tailored to optimally address the consequences of AHR disruption at critical times of the cardiogenesis program. Maternal exposure to TCDD at E7.5 impacts the induction of cardiogenic mesoderm from splanchnic

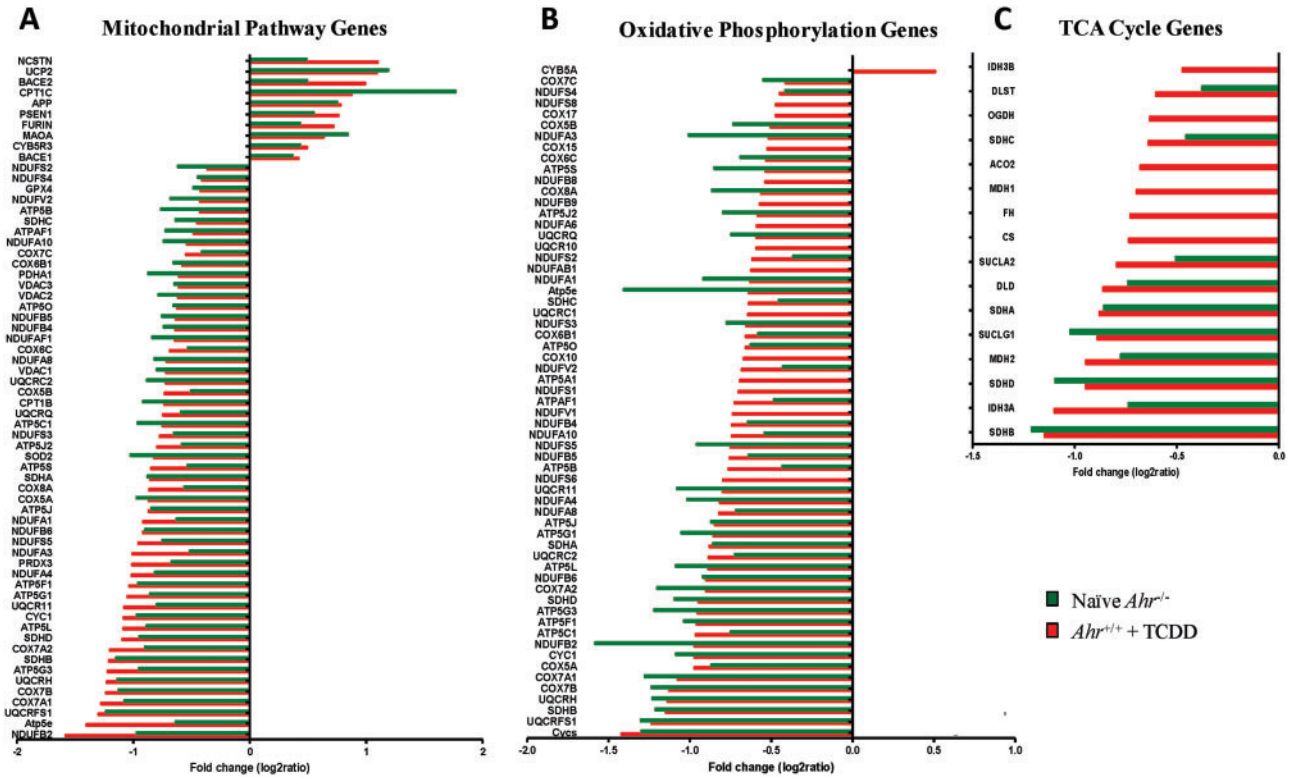

FIG. 6. Disruption of AHR signaling perturbs the regulation of molecular networks that control mitochondrial function during development. Fold change of expression of significantly altered genes in (A) functional mitochondrial pathways; B, oxidative phosphorylation, and C, TCA cycle in E15.5 right atrium of ligand-exposed $Ahr^{+/+}$ (*red*) and $Ahr^{-/-}$ (*green*) embryo hearts. Full color version available online.

mesoderm and the critical initiation events in cellular commitment toward cardiomyogenesis. Treatment at E9.5 and E11.5 impinges on the formation of atria and ventricles from the elongated and looped heart tube that needs to further proliferate and mature prior to chamber septation (de Boer *et al.*, 2012). AHR disruption during these critical events, be it from ablation or by ligand-induced downregulation, provided the means to characterize the role of the AHR in gene-environment interactions in cardiogenesis.

Consistent with a lack of overt systemic embryo toxicity, no effects to litter size or embryo body weight were observed. Yet, the AHR/TCDD axis had a significant role in the gross anatomical development of the heart, causing a significant decrease of total ventricle thickness at weight at late gestation. AHR ligand exposure also altered the composition of the ventricular wall, increasing the thickness of the compact myocardium and reducing the total myocardial mass, as previously reported (Thackaberry *et al.*, 2005). These morphological changes paralleled increases in cell proliferation at E13.5 and E18.5, possibly representing a compensatory mechanism to rescue a decrease cell proliferation rate prior to E13.5. Conversely, *Ahr* gene ablation resulted in decreased cell proliferation across all developmental time points measured, perhaps as part of the mechanism underlying the decreased heart weight and wall thickness associated with constitutive ablation of the receptor. Ultimately, disruption of endogenous AHR functions *in utero* and structural abnormalities correlated with echocardiographic alterations of fetal heart function, characterized by higher heart rates in ligand exposed embryos and right and left ventricle dilation resulting in higher stroke volume though reduced ejection fraction in knockout embryos.

In line with our findings in ES cells (Wang *et al.*, 2013), the AHR is mostly nuclear in the developing mouse heart in a high percentage of cells at E13.5 and E15.5, even in the absence of an exogenous ligand. At this time, however, the localization appears to be mainly in cells lining the internal and external surfaces of the developing myocardium, endocardium, and epicardium, respectively, and most consistent with an endothelial identity. In contrast, at E18.5, the localization is predominantly cytoplasmic in cardiac troponin T-positive cardiomyocytes, in agreement with its localization in many tissue culture cell lines and adult mouse liver. At the earlier time points, ligand exposure decreased the level of nuclear localization, conceivably by export from the nucleus and proteasomal degradation, as shown in *in vitro* systems (Schmidt and Bradfield, 1996). These results strengthen the view that at early development times the AHR has an endogenous function that may be a target for disruption by exposure to exogenous ligands, such as TCDD. AHR nuclear localization may be the consequence of activation by endogenous mechanisms, either ligand-independent or dependent on an endogenous ligand. In either case, it appears that the AHR may have a role in heart development that is independent of exogenous ligand-mediated activation and that TCDD, an exogenous ligand, may sequester it away from its endogenous function. While the AHR is a recognized hub in gene/environment interactions, the developmental spatial and temporal patterns of AHR expression have been only partially identified in mammals (Abbott *et al.*, 1995; Kitajima *et al.*, 2004). The AHR subcellular location during development is incompletely characterized, loosely described as either cytoplasmic, nuclear, or a combination thereof in a time, cell/tissue, and ligand-binding status dependent fashion. Thus, the

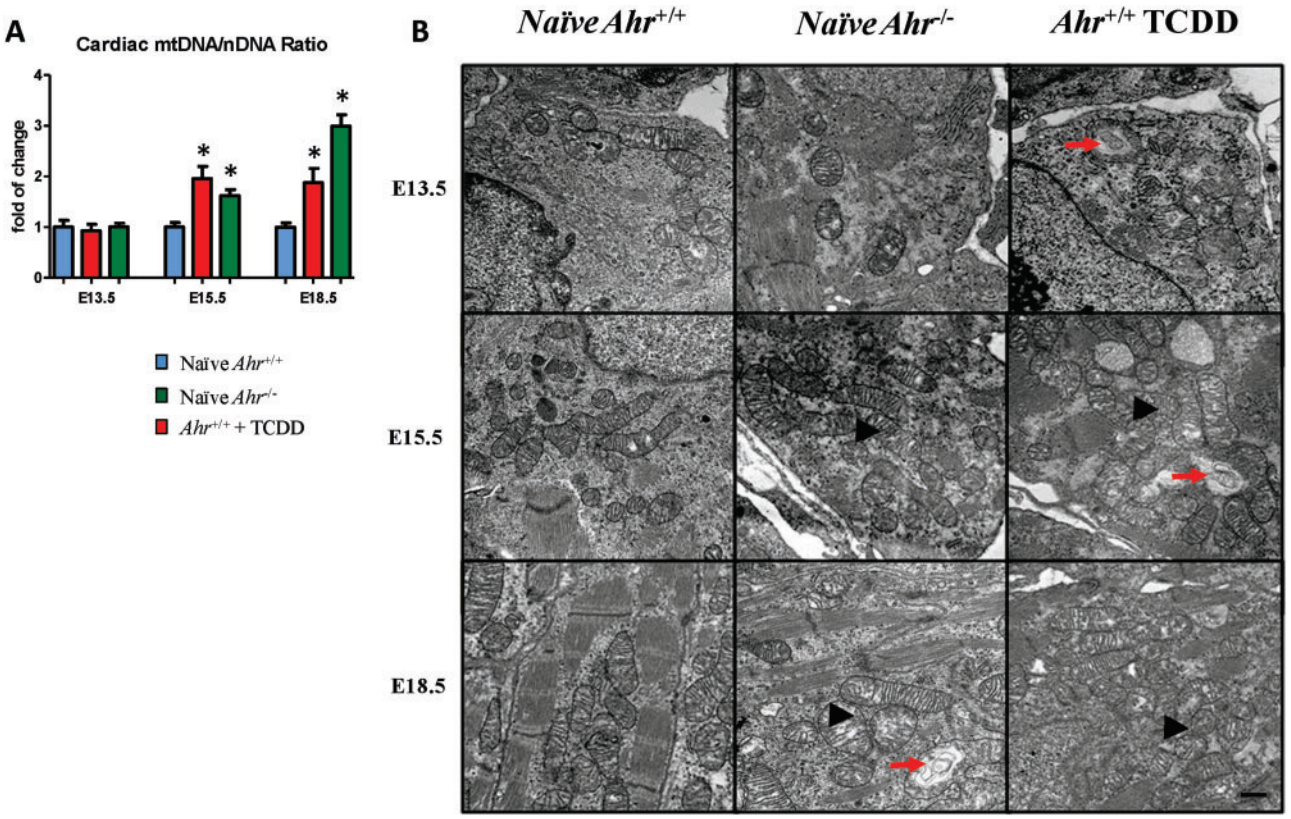

FIG. 7. Disruption of AHR signaling induces changes in mitochondria abundance and structure. A, Quantification of heart mitochondrial DNA relative to nuclear DNA, defined as the ratio of mtDNA to nDNA ratio at E13.5, E15.5, and E18.5 and expressed as the mean fold change relative to naïve $Ahr^{+/+}$ hearts ± SEM; $^{*}P \leq .05$. B, Ultrathin sections of embryonic hearts collected at E13.5, E15.5, and E18.5 from $Ahr^{-/-}$ and $Ahr^{+/+}$, either naïve or exposed to ligand *in utero*, were used for transmission electron microscopy evaluation of the embryonic heart ultrastructure. Representative photomicrographs illustrating higher density of mitochondria (*arrowheads*) within the embryonic cardiomyocyte sarcoplasm in $Ahr^{-/-}$ and in ligand-exposed $Ahr^{+/+}$ compared with naïve $Ahr^{+/+}$. Individual or clusters of mitochondria showed ultrastructural features of stress and degeneration (*arrows*), as evidenced by focal to global swelling, loss of matrix density, as well as cristae unpacking, disorganization, and cristolysis, affecting a higher number of mitochondria in AHR ligand-exposed $Ahr^{+/+}$ hearts. Uranyl acetate and lead citrate stain. Scale bar = 500 nm.

homeostatic pattern of AHR expression in naïve tissues delineated in this study advances our understanding of the contributions of this protein to cardiac morphogenesis and physiology (Puga, 2011; Zhang, 2011).

The hearts of $Ahr^{-/-}$ and ligand-exposed embryos showed decreased nuclear expression of the cardiogenesis regulator NKX2-5, as previously observed *in vitro* (Puga, 2011; Zhang, 2011). This is of particular importance as decreased expression of the *Nkx2-5* gene, in and of itself, brings about haploinsufficiency of its product, with resultant pathological phenotypes such as CHD and cardiomyopathies (Prall *et al.*, 2007). *In utero* AHR disruption not only repressed *Nkx2-5* expression but also derailed the expression of NKX2-5 regulated genes and of genes controlling pathways responsible for attainment and maintenance of cardiac differentiation, homeostasis, and function. For the most part, the identity and direction of the resulting gene expression changes were strikingly similar between $Ahr^{-/-}$ and ligand-exposed $Ahr^{+/+}$ embryos and were annotated to ontogenies of cardiogenesis, cardiac function, congenital heart anomaly, homeobox transcription factors, AHR signaling, NKX2-5 signaling, and isoproterenol response (ie, functional stress) pathways, all central to cardiomyocyte homeostasis.

In addition to the effects in cardiogenesis pathways and NKX2-5 signaling, disruption of endogenous AHR signaling, either by ablation or by TCDD exposure, also down-regulated the expression of genes encoding subunits of all 5 mitochondrial respiratory chain (MRC) complexes and other genes regulating oxidative phosphorylation and the TCA cycle, all playing a central role in essential biological processes through the generation of reactive oxygen and production of cellular energy. AHR disruption has previously been shown to cause mitochondrial dysfunction (Kennedy *et al.*, 2013; Pereira *et al.*, 2013; Senft *et al.*, 2002; Tappenden *et al.*, 2011) with resulting altered expression of nuclear encoded mitochondrial genes (Forgacs *et al.*, 2010) and increased abundance of mitochondria (Kim *et al.*, 2013; Pavanello *et al.*, 2013). Mitochondrial defects have been implicated in various diseases, including cardiovascular disease (Pereira *et al.*, 2013; Wallace, 2013), but less is known about how they specifically impact the mechanisms involved in early embryonic development. Knockout of the mitochondrial *Tfam* transcription factor A is known to block transcription of all 13 mitochondrial DNA-encoded MRC subunits, causing embryonic lethality (Larsson *et al.*, 1998). In our experiments, while AHR disruption is not embryonic lethal, repression of complex V components, particularly ATP5α1, a subunit of the ATP synthase complex, may be responsible for the mitochondria dysfunction resulting from loss of AHR signaling, since AHR can directly interact with ATP5α1 and modulate mitochondrial function (Tappenden *et al.*, 2011). At any rate, given the extent of the resulting gene expression changes, we might expect that energy balance, including ATP yield, protonmotive force, respiratory rate, and mitochondrial membrane potential will be perturbed by AHR disruption, causing a compensatory increase of aerobic glycolysis in the cytoplasm,

accompanied by formation of lactate from pyruvate. Although cardiomyocytes can efficiently produce energy from lactate (Tohyama *et al.*, 2013), tight regulation of energy generation and handling is paramount for the maintenance of heart homeostasis and is likely to be impaired by AHR disruption. Ultimately, mitochondrial dysfunction from AHR disruption *in utero* results in ultrastructural alterations suggestive of mitochondrial stress and degeneration and increased mitochondria abundance within the heart, most likely as a compensatory effect of the loss of efficiency of individual mitochondria.

Our observations strongly indicate that developmental disruption of AHR function causes covert cardiac morphological and functional effects due to, or accompanied by, many dysregulated signaling pathways involved in cardiogenesis, cardiac function, and metabolism, which, collectively, are likely to deter postnatal cardiovascular function. Whether embryonic disruption of AHR pathways causes adult cardiac insufficiency is yet to be determined. The results presented here provide strong evidence in support of a central role for the AHR signaling network in heart development, where the AHR is also a target of environmental agents that can cause departure from homeostasis and underlie CHD. These findings underscore the AHR as a key contributor to heart development and homeostasis and increase our understanding of environmental cardiac injury and its prevention.

SUPPLEMENTARY DATA

Supplementary data are available online at http://toxsci.oxfordjournals.org/.

FUNDING

National Institute of Environmental Health Sciences (NIEHS) (R01 ES06273, R01 ES024744, and R01 ES10807), and by the NIEHS Center for Environmental Genetics (P30 ES06096). NIEHS Gene–Environment Interactions Training (T32 ES016646 to V.C.).

REFERENCES

Abbott, B. D., Birnbaum, L. S., and Perdew, G. H. (1995). Developmental expression of two members of a new class of transcription factors: I. Expression of aryl hydrocarbon receptor in the C57BL/6N mouse embryo. *Dev. Dyn.* **204**, 133–143.

Abbott, B. D., Schmid, J. E., Pitt, J. A., Buckalew, A. R., Wood, C. R., Held, G. A., and Diliberto, J. J. (1999). Adverse reproductive outcomes in the transgenic Ah receptor-deficient mouse. *Toxicol. Appl. Pharmacol.* **155**, 62–70.

Aragon, A. C., Kopf, P. G., Campen, M. J., Huwe, J. K., and Walker, M. K. (2008). In utero and lactational 2,3,7,8-tetrachlorodibenzo-p-dioxin exposure: effects on fetal and adult cardiac gene expression and adult cardiac and renal morphology. *Toxicol. Sci.* **101**, 321–330.

Barker, D. J. (2007). The origins of the developmental origins theory. *J. Int. Med.* **261**, 412–417.

Carro, T., Dean, K., and Ottinger, M. A. (2013). Effects of an environmentally relevant polychlorinated biphenyl (PCB) mixture on embryonic survival and cardiac development in the domestic chicken. *Environ.Toxicol. Chem.* **32**, 1325–1331.

Dabir, P., Marinic, T. E., Krukovets, I., and Stenina, O. I. (2008). Aryl hydrocarbon receptor is activated by glucose and regulates the thrombospondin-1 gene promoter in endothelial cells. *Circ. Res.* **102**, 1558–1565.

Dalton, T., Kerzee, J., Wang, B., Miller, M., Dieter, M., Lorenz, J., Shertzer, H., Nebert D.W., and Puga, A. (2001). Dioxin exposure is an environmental risk factor for ischemic heart disease. *Cardiovasc. Toxicol.* **1**, 285–298.

Davarinos, N. A., and Pollenz, R. S. (1999). Aryl hydrocarbon receptor imported into the nucleus following ligand binding is rapidly degraded via the cytosplasmic proteasome following nuclear export. *J. Biol. Chem.* **274**, 28708–28715.

de Boer, B. A., van den Berg, G., de Boer, P. A., Moorman, A. F., and Ruijter, J. M. (2012). Growth of the developing mouse heart: an interactive qualitative and quantitative 3D atlas. *Dev. Biol.* **368**, 203–213.

Forgacs, A. L., Burgoon, L. D., Lynn, S. G., LaPres, J. J., and Zacharewski, T. (2010). Effects of TCDD on the expression of nuclear encoded mitochondrial genes. *Toxicol. Appl. Pharmacol.* **246**, 58–65.

Furness, S. G., Lees, M. J., and Whitelaw, M. L. (2007). The dioxin (aryl hydrocarbon) receptor as a model for adaptive responses of bHLH/PAS transcription factors. *FEBS Lett.* **581**, 3616–3625.

Furness, S. G., and Whelan, F. (2009). The pleiotropy of dioxin toxicity–xenobiotic misappropriation of the aryl hydrocarbon receptor's alternative physiological roles. *Pharmacol. Therap.* **124**, 336–353.

Giannone, J. V., Li, W., Probst, M., and Okey, A. B. (1998). Prolonged depletion of AH receptor without alteration of receptor mRNA levels after treatment of cells in culture with 2,3,7,8-tetrachlorodibenzo-p-dioxin. *Biochem. Ppharmacol.* **55**, 489–497.

Hinton, R. B. (2013). Genetic and environmental factors contributing to cardiovascular malformation: a unified approach to risk. *J. Am. Heart Assoc.* **2**, e000292–e000295.

Hofsteen, P., Mehta, V., Kim, M. S., Peterson, R. E., and Heideman, W. (2013). TCDD inhibits heart regeneration in adult zebrafish. *Toxicol. Sci.* **132**, 211–221.

Jones, S. P., and Kennedy, S. W. (2009). Chicken embryo cardiomyocyte cultures—a new approach for studying effects of halogenated aromatic hydrocarbons in the avian heart. *Toxicol. Sci.* **109**, 66–74.

Kennedy, L. H., Sutter, C. H., Leon, C. S., Tran, Q. T., Bodreddigari, S., Kensicki, E., Mohney, R. P., and Sutter, T. R. (2013). 2,3,7,8-Tetrachlorodibenzo-p-dioxin-mediated production of reactive oxygen species is an essential step in the mechanism of action to accelerate human keratinocyte differentiation. *Toxicol. Sci.* **132**, 235–249.

Kewley, R. J., Whitelaw, M. L., and Chapman-Smith, A. (2004). The mammalian basic helix-loop-helix/PAS family of transcriptional regulators. *Int. J. Biochem. Cell Biol.* **36**, 189–204.

Kim, H. Y., Kim, H. R., Kang, M. G., Trang, N. T., Baek, H. J., Moon, J. D., Shin, J. H., Suh, S. P., Ryang, D. W., Kook, H., *et al.* (2013). Profiling of biomarkers for the exposure of polycyclic aromatic hydrocarbons: lamin-A/C isoform 3, poly[ADP-ribose] polymerase 1, and mitochondria copy number are identified as universal biomarkers. *BioMed. Res. Int.* **2014**, 605135.

Kitajima, M., Khan, K. N., Fujishita, A., Masuzaki, H., Koji, T., and Ishimaru, T. (2004). Expression of the arylhydrocarbon receptor in the peri-implantation period of the mouse uterus and the impact of dioxin on mouse implantation. *Arch. Histol. Cytol.* **67**, 465–474.

Lage, K., Greenway, S. C., and Rosenfeld, J. A. (2012). Genetic and environmental risk factors in congenital heart disease

functionally converge in protein networks driving heart development. *Proc. Natl. Acad. Sci. U.S.A.* **109**, 14035–14040.

Larsson, N. G., Wang, J., Wilhelmsson, H., Oldfors, A., Rustin, P., Lewandoski, M., Barsh, G. S., and Clayton, D. A. (1998). Mitochondrial transcription factor A is necessary for mtDNA maintenance and embryogenesis in mice. *Nat. Genetics* **18**, 231–236.

Li, X., Martinez-Fernandez, A., Hartjes, K. A., Kocher, J. P., Olson, T. M., Terzic, A., and Nelson, T. J. (2014). Transcriptional atlas of cardiogenesis maps congenital heart disease interactome. *Physiol. Genomics* **46**, 482–495.

Lints, T. J., Parsons, L. M., Hartley, L., Lyons, I., and Harvey, R. P. (1993). Nkx-2.5: a novel murine homeobox gene expressed in early heart progenitor cells and their myogenic descendants. *Development* **119**, 419–431.

Lund, A. K., Agbor, L. N., Zhang, N., Baker, A., Zhao, H., Fink, G. D., Kanagy, N. L., and Walker, M. K. (2008). Loss of the aryl hydrocarbon receptor induces hypoxemia, endothelin-1, and systemic hypertension at modest altitude. *Hypertension* **51**, 803–809.

Mongan, M., Tan, Z., Chen, L., Peng, Z., Dietsch, M., Su, B., Leikauf, G., and Xia, Y. (2008). Mitogen-activated protein kinase kinase kinase 1 protects against nickel-induced acute lung injury. *Toxicol. Sci.* **104**, 405–411.

Nora, J. J. (1968). Multifactorial Inheritance hypothesis for the etiology of congenital heart diseases: the genetic-environmental interaction. *Circulation* **38**, 604–617.

Pavanello, S., Dioni, L., Hoxha, M., Fedeli, U., Mielzynska-Svach, D., and Baccarelli, A. (2013). Mitochondrial DNA copy number and exposure to polycyclic aromatic hydrocarbons. *Cancer Epidemiol. Biomark. Prev.* **22**, 1722–1729.

Pereira, S. P., Pereira, G. C., Pereira, C. V., Carvalho, F. S., Cordeiro, M. l. H., Mota, P. C., Ramalho-Santos, J., Moreno, A. N. J., and Oliveira, P. J. (2013). Dioxin-induced acute cardiac mitochondrial oxidative damage and increased activity of ATP-sensitive potassium channels in Wistar rats. *Environ. Pollut.* **180**, 281–290.

Prall, O. W., Menon, M. K., Solloway, M. J., Watanabe, Y., Zaffran, S. P., Bajolle, F., Biben, C., McBride, J. J., Robertson, B. R., Chaulet, H., *et al.* (2007). An Nkx2-5/Bmp2/Smad1 negative feedback loop controls heart progenitor specification and proliferation. *Cell* **128**, 947–959.

Puga, A. (2011). Perspectives on the potential involvement of the AH receptor-dioxin axis in cardiovascular disease. *Toxicol. Sci.* **120**, 256–261.

Puga, A., Ma, C., and Marlowe, J. L. (2009). The aryl hydrocarbon receptor cross-talks with multiple signal transduction pathways. *Biochem. Pharmacol.* **77**, 713–722.

Quintana, F. J., and Sherr, D. H. (2013). Aryl hydrocarbon receptor control of adaptive immunity. *Pharmacol. Rev.* **65**, 1148–1161.

Rana, M. S., Christoffels, V. M., and Moorman, A. F. (2013). A molecular and genetic outline of cardiac morphogenesis. *Acta Physiol.* **207**, 588–615.

Sauzeau, V., Carvajal-González, J. M., Riolobos, A. S., Sevilla, M. A., Menacho-Márquez, M., Román, A. C., Abad, A., Montero, M. J., Fernández-Salguero, P., and Bustelo, X. R. (2011). Transcriptional factor aryl hydrocarbon receptor (Ahr) controls cardiovascular and respiratory functions by regulating the expression of the Vav3 proto-oncogene. *J. Biol. Chem.* **286**, 2896–2909.

Schmidt, J. V., and Bradfield, C. A. (1996). Ah receptor signaling pathways. *Annu. Rev. Cell Dev. Biol.* **12**, 55–89.

Scholzen, T., and Gerdes, J. (2000). The Ki-67 protein: from the known and the unknown. *J. Cell. Physiol.* **182**, 311–322.

Schwartz, R., and Olson, E. (1999). Building the heart piece by piece: modularity of cis-elements regulating Nkx2-5 transcription. *Development* **126**, 4187–4192.

Senft, A. P., Dalton, T. P., Nebert, D. W., Genter, M. B., Puga, A., Hutchinson, R. J., Kerzee, J. K., Uno, S., and Shertzer, H. G. (2002). Mitochondrial reactive oxygen production is dependent on the aromatic hydrocarbon receptor. *Free Radic. Biol. Med.* **33**, 1268–1278.

Srinivasan, S., Baldwin, H. S., Aristizabal, O., Kwee, L., Labow, M., Artman, M., and Turnbull, D. H. (1998). Noninvasive, in utero imaging of mouse embryonic heart development with 40-MHz echocardiography. *Circulation* **98**, 912–918.

Srivastava, D., and Olson, E. (2000). A genetic blueprint for cardiac development. *Nature* **407**, 221–226.

Stites, T., Storms, D., Bauerly, K., Mah, J., Harris, C., Fascetti, A., Rogers, Q., Tchaparian, E., Satre, M., and Rucker, R. B. (2006). Pyrroloquinoline quinone modulates mitochondrial quantity and function in mice. *J. Nutr.* **136**, 390–396.

Tappenden, D. M., Lynn, S. G., Crawford, R. B., Lee, K., Vengellur, A., Kaminski, N. E., Thomas, R. S., and LaPres, J. J. (2011). The aryl hydrocarbon receptor interacts with ATP5(1, a subunit of the ATP synthase complex, and modulates mitochondrial function. *Toxicol. Appl. Pharmacol.* **254**, 299–310.

Thackaberry, E. A., Nunez, B. A., Ivnitski-Steele, I. D., Friggins, M., and Walker, M. K. (2005). Effect of 2,3,7,8-tetrachlorodibenzo-p-dioxin on murine heart development: alteration in fetal and postnatal cardiac growth, and postnatal cardiac chronotropy. *Toxicol. Sci.* **88**, 242–249.

Tohyama, S., Hattori, F., Sano, M., Hishiki, T., Nagahata, Y., Matsuura, T., Hashimoto, H., Suzuki, T., Yamashita, H., Satoh, Y., *et al.* (2013). Distinct metabolic flow enables large-scale purification of mouse and human pluripotent stem cell-derived cardiomyocytes. *Cell Stem Cell* **12**, 127–137.

van der Bom, T., Zomer, C. A., Zwinderman, A. H., Meijboom, F. J., Bouma, B. J., and Mulder, B. J. (2011). The changing epidemiology of congenital heart disease. *Nat. Rev. Cardiol.* **8**, 50–60.

Van Vliet, P., Wu, S. M., Zaffran, S. P., and Puceat, M. (2012). Early cardiac development: a view from stem cells to embryos. *Cardiovasc. Res.* **96**, 352–362.

Vecoli, C., Pulignani, S., and Foffa, I. (2014). Congenital heart disease: the crossroads of genetics, epigenetics and environment. *Curr. Genomics* **15**, 390–399.

Wallace, D. C. (2013). A mitochondrial bioenergetic etiology of disease. *J. Clin. Invest.* **123**, 1405–1412.

Wang, Q., Chen, J., Ko, C. I. I., Fan, Y., Carreira, V., Chen, Y., Xia, Y., Medvedovic, M., and Puga, A. (2013). Disruption of aryl hydrocarbon receptor homeostatic levels during embryonic stem cell differentiation alters expression of homeobox transcription factors that control cardiomyogenesis. *Environ. Health Perspect.* **121**, 1334–1343.

Weber, H., and Birnbaum, L. S. (1985). 2,3,7,8-Tetrachlorodibenzo-p-dioxin (TCDD) and 2,3,7,8-tetrachlorodibenzofuran (TCDF) in pregnant C57BL/6N mice: distribution to the embryo and excretion. *Arch. Toxicol.* **57**, 159–162.

Yoshioka, W., Peterson, R. E., and Tohyama, C. (2011). Molecular targets that link dioxin exposure to toxicity phenotypes. *J. Steroid Biochem. Mol. Biol.* **127**, 96–101.

Zhang, N. (2011). The role of endogenous aryl hydrocarbon receptor signaling in cardiovascular physiology. *J. Cardiovasc. Dis. Res.* **2**, 91–95.